Journal of Pathology
J Pathol 2020; **250:** 374–386
Published online 4 February 2020 in Wiley Online Library (wileyonlinelibrary.com) DOI: 10.1002/path.5379

ORIGINAL PAPER

Hippo pathway effectors YAP1/TAZ induce an *EWS–FLI1*-opposing gene signature and associate with disease progression in Ewing sarcoma

Pablo Rodríguez-Núñez[1†,‡], Laura Romero-Pérez[2†,‡*], Ana T Amaral[1,3], Pilar Puerto-Camacho[1], Carmen Jordán[1], David Marcilla[1], Thomas GP Grünewald[2,4,5], Javier Alonso[6,7], Enrique de Alava[1,3,8*] and Juan Díaz-Martín[1,3‡*]

[1] *Department of Pathology, Hospital Universitario Virgen del Rocío, Instituto de Biomedicina de Sevilla, CSIC-Universidad de Sevilla, Seville, Spain*
[2] *Max-Eder Research Group for Pediatric Sarcoma Biology, Institute of Pathology, Faculty of Medicine, Munich, Germany*
[3] *Centro de Investigación Biomédica en Red de Cáncer, Instituto de Salud Carlos III, Madrid, Spain*
[4] *German Cancer Consortium (DKTK), Munich, Germany*
[5] *German Cancer Research Center (DKFZ), Heidelberg, Germany*
[6] *Unidad de Tumores Sólidos Infantiles, Instituto de Investigación de Enfermedades Raras, Instituto de Salud Carlos III, Madrid, Spain*
[7] *Centro de Investigación Biomédica en Red de Enfermedades Raras, Instituto de Salud Carlos III (CB06/07/1009; CIBERER-ISCIII), Madrid, Spain*
[8] *Department of Normal and Pathological Cytology and Histology, School of Medicine, University of Seville, Seville, Spain*

**Correspondence to: L Romero-Pérez, Max Eder Research Group for Pediatric Sarcoma Biology, Institute of Pathology, Thalkirchner Str. 36, 80337 Munich, Germany. E-mail: lromero-ibis@us.es, laura.romeroperez@med.uni-muenchen.de; Or E de Álava, Instituto of Biomedicine of Sevilla (IBiS), Lab. 203 (Patología Molecular), Av. Manuel Siurot s/n, 41013-Sevilla, Spain. E-mail: enrique.alava.sspa@juntadeandalucia.es; Or J Díaz-Martín, Instituto of Biomedicine of Sevilla (IBiS), Lab. 203 (Patología Molecular), Av. Manuel Siurot s/n 41013-Sevilla, Spain. E-mail: jdiaz-ibis@us.es*

[†]Co-first authorship.
[‡]These authors contributed equally to this work.

Abstract

YAP1 and TAZ (WWTR1) oncoproteins are the final transducers of the Hippo tumor suppressor pathway. Deregulation of the pathway leads to YAP1/TAZ activation fostering tumorigenesis in multiple malignant tumor types, including sarcoma. However, oncogenic mutations within the core components of the Hippo pathway are uncommon. Ewing sarcoma (EwS), a pediatric cancer with low mutation rate, is characterized by a canonical fusion involving the gene *EWSR1* and *FLI1* as the most common partner. The fusion protein is a potent driver of oncogenesis, but secondary alterations are scarce, and little is known about other biological factors that determine the risk of relapse or progression. We have observed YAP1/TAZ expression and transcriptional activity in EwS cell lines. Analyses of 55 primary human EwS samples revealed that high YAP1/TAZ expression was associated with progression of the disease and predicted poorer outcome. We did not observe recurrent SNV or copy number gains/losses in Hippo pathway-related loci. However, differential CpG methylation of the *RASSF1* locus (a regulator of the Hippo pathway) was observed in EwS cell lines compared with mesenchymal stem cells, the putative cell of origin of EwS. Hypermethylation of *RASSF1* correlated with the transcriptional silencing of the tumor suppressor isoform *RASFF1A*, and transcriptional activation of the pro-tumorigenic isoform *RASSF1C*, which promotes YAP1/TAZ activation. Knockdown of YAP1/TAZ decreased proliferation and invasion abilities of EwS cells and revealed that YAP1/TAZ transcription activity is inversely correlated with the EWS–FLI1 transcriptional signature. This transcriptional antagonism could be explained partly by EWS–FLI1-mediated transcriptional repression of TAZ. Thus, YAP1/TAZ may override the transcriptional program induced by the fusion protein, contributing to the phenotypic plasticity determined by dynamic fluctuation of the fusion protein, a recently proposed model for disease dissemination in EwS.

Keywords: Ewing sarcoma; Hippo pathway; metastasis; immunohistochemistry; transcriptional signatures

Received 16 July 2019; Revised 26 November 2019; Accepted 20 December 2019

No conflicts of interest were declared.

Introduction

Ewing sarcoma (EwS) represents the second most common primary malignant bone tumor in children and young adults [1]. Owing to multimodal treatment concepts, 2/3 of patients with localized disease achieve sustained remission but approximately 30% relapse. Patients at relapse or with advanced disease have limited

chance to survive, with a 3-year event-free survival of less than 25% [2,3]. While clinical prognostic markers such as the presence of metastases or tumor volume are established, little is known about the biological factors determining the risk of progression, thus precluding risk-adapted therapeutic approaches. EwS was the first solid malignancy defined by the presence of tumor-specific *EWSR1–ETS* gene fusions [4], mainly *EWSR1–FLI1* translocations, which are considered the main driver of the disease, but fusion type itself does not have any impact on disease progression [5]. As in most developmental cancers, additional recurrent mutations are scarce. The most common somatic mutations have been detected in *STAG2*, *CDKN2A*, and *TP53*, associated with poor prognosis [6,7]. Copy number variation studies by the PROVABES Consortium using samples derived from the EURO-E.W.I.N.G. 99 (EE99) and EWING 2008 trials showed that chromosome 1q gain and possibly chromosome 16q loss define patients with a poor clinical outcome (Díaz-Martín *et al*, unpublished data), supporting previous retrospective studies [7,8]. However, these secondary alterations occur with a frequency that does not account for the large proportion of patients who relapse.

The Hippo tumor suppressor pathway plays a critical role in tissue and organ size regulation by restraining cell proliferation and apoptosis under homeostatic conditions [9]. Central to the Hippo pathway is a conserved cascade of adaptor proteins and inhibitory kinases that regulate the activity of the oncoproteins YAP1 and TAZ, the final effectors of this pathway in mammals. YAP1/TAZ do not directly bind to DNA, but act as transcriptional coactivators of target genes involved in cell proliferation and survival through their interaction with transcriptional regulators such as TEAD factors [10]. The role of YAP1 and TAZ as important drivers in tumorigenesis has been extensively reported in carcinomas, and they also contribute to malignancies of mesenchymal origin [11–13]. In fact, given its key function in developmental processes, an important role has been inferred for Hippo signaling in pediatric cancer [14]. Despite this, somatic or germline mutations in Hippo pathway genes are uncommon, in comparison to other well-defined signaling pathways that are commonly disrupted in cancer [13,15]. Since secondary genetic alterations are scarce in EwS and given the established role of YAP1 and TAZ in cancer without engaging mutation, we aimed to explore the contribution of these factors to oncogenesis in EwS. Herein, we evaluated a series of 55 EwS patients by immunohistochemistry (IHC) for expression/activation of YAP1 and TAZ. We observed a significant association of YAP1/TAZ nuclear expression and disease progression, as well as a potential mechanism of dysregulation involving epigenetic regulation of the *RASSF1* locus. Moreover, we demonstrated an interesting interplay between TAZ/YAP1 function with the fusion protein, which fits into a recent model concept for metastatic spreading in EwS based on fluctuations of the expression of the fusion protein [16].

Materials and methods

Tumor samples, TMA construction, and immunohistochemistry (IHC)

Tissue samples were obtained from the HUVR-IBiS Biobank (Universitary Hospital Virgen del Rocio–Institute of Biomedicine of Seville Biobank, Andalusian Public Health System Biobank). This study was performed following standard Spanish ethical regulations and was approved by the corresponding ethics committee of the Hospital Virgen del Rocío de Sevilla and the Fundación Pública Andaluza para la Gestión de la Investigación en Salud de Sevilla (FISEVI), Spain. Written informed consent was obtained from all patients and all clinical analyses were conducted in accordance with the principles of the Declaration of Helsinki.

In this study, we analyzed 88 formalin-fixed, paraffin-embedded (FFPE) samples from 68 different EwS patients (55 samples corresponding to primary tumor). We also analyzed a subset of 21 frozen samples from the same series (17 primary tumors and four metastasis). Clinical diagnosis of all the samples was performed according to the World Health Organization (WHO) classification [17], performing fluorescence *in situ* hybridization (FISH) to assess the presence of EwS translocation in tissue sections. The only selection criteria were the availability of pathological data and tissue for tissue microarray (TMA) construction. Medical records were retrospectively reviewed and clinicopathologic information for 55 patients with primary tumor material was retrieved for further analyses (summarized in Table 1).

Representative tumor areas of EwS samples were selected on H&E-stained sections and two 1-mm diameter tissue cores were obtained from each specimen to set up four different TMAs. IHC was carried out on TMA sections using the Envision method (Dako, CA, USA) with a step of heat-induced antigen retrieval and using a primary antibody against YAP1 and TAZ (supplementary material, Table S1). YAP1/TAZ nuclear staining was separately evaluated by two pathologists. Tissue was given a score which resulted from multiplying the nuclear staining intensity from 0 (no staining) to 3 (strong staining) by the extension based on the percentage from positive cells (from 0 to 3). Samples were grouped as negative or weak positive (score 0–2), and strong positive (3–9).

Cell culture and transfection

EwS cell lines SKNMC, TTC-466, TC32, A4573, A673, CADO-ES, RD-ES, RM82, SKES1, STAET10, TC71, and WE68 were obtained from the EuroBoNet cell line panel [18]. MDA-MB-231, MCF7, RH30, SA-OS-2, and PC3 cell lines were purchased from the ATCC

Table 1. Clinical and pathologic findings according to YAP1/TAZ nuclear expression in primary EwS specimens (n = 55)

Characteristics	Analyzable	YAP1/TAZ expression (IHC)		p
		Negative/weak positive	Strong positive	
Age (years) mean	**55**	20.72 (±2.062)	20.93 (±3.196)	0.9088
Location	**42**			0.4945
Bone	28 (66.67%)	19 (67.86%)	9 (32.14%)	
Soft tissue	14 (33.33%)	8 (57.14%)	6 (42.86%)	
Progression	**50**			**0.0054**
No	27 (54%)	21 (77.78%)	6 (22.22%)	
Yes	23 (46%)	9 (39.13%)	14 (60.87%)	

p value in bold indicates a significant association ($p < 0.05$) of YAP1/TAZ staining with the corresponding characteristic.

(Manassas, VA, USA). All tumor cell lines were authenticated by short tandem repeat analyses (CLS, Germany). Primary human bone marrow mesenchymal cells (hMSCs), immortalized with telomerase reverse transcriptase, were provided by D Campana [19]. The A673 cell line engineered to express a doxycycline-inducible shRNA against *EWS–FLI1* was kindly provided by J Alonso [20]. For the *EWS–FLI1* shRNA induction, 1 µg/ml doxycycline (D9891; Sigma, St Louis, MO, USA) was added to the media for 48 h. Detailed information of the immunofluorescence, siRNA silencing, Crispr KO, luciferase reporter assays, cell migration, and invasion protocols are described in supplementary material, Supplementary materials and methods.

Genome-wide copy number analysis

FFPE samples were sliced into 10-µm-thick sections and genomic DNA (gDNA) was extracted using the QIAamp DNA FFPE Tissue Kit (Qiagen, Crawley, UK). DNA concentration was determined using the Quant-iT™ PicoGreenR dsDNA Assay Kit (Thermo Fisher Scientific, Waltham, MA, USA). Genome-wide copy number analysis was performed using the OncoScan FFPE Assay Kit (Affymetrix, Santa Clara, CA, USA) according to the manufacturer's recommendations. Nexus Express for OncoScan 3 software (BioDiscovery, Hawthorne, CA, USA) was used to estimate copy numbers. The significance testing for aberrant copy number (STAC) method was conducted to evaluate the significance of DNA copy number aberrations across the tumor series.

Methylation array

Methylation data were generated as described in Puerto-Camacho *et al* [21]. Data analyses of GSE118872 were performed using the Bioconductor lumi package [22].

Transcriptome analysis

SK-N-MC cells were transfected with control or a combination of *YAP1/TAZ* siRNAs for 72 h. Whole transcript expression analysis was conducted in four biological replicates of each sample. A 100 ng aliquot of total RNA was amplified using the GeneChip® WT PLUS reagent kit (Thermo Fisher Scientific) following the manufacturer's instructions. The amplified cDNA was quantified, fragmented, and labeled in preparation for hybridization to GeneChip® Human Transcriptome 2.0 Array (Thermo Fisher Scientific) using 5.5 µg of single-stranded cDNA product and following protocols outlined in the user manual. CHP files were analyzed by Transcriptome Analysis Console (TAC) 4.0 software (Thermo Fisher Scientific), which performs statistical analysis and provides a list of differentially expressed genes. Gene set enrichment analysis (GSEA v3.0) was performed to identify targets of YAP1/TAZ that were over-represented in previous defined gene sets [23,24].

Statistical analyses

Correlation between immunohistochemical YAP1/TAZ expression and clinicopathological characteristics was assessed by chi-squared test for the categorical variables. The Mann–Whitney test was used for the analysis of differences of the continuous variable age. EwS-specific survival was defined as the time from surgery to the time of death from EwS, with deaths from other causes being censored, whereas in time to relapse analysis, the end point was EwS recurrence, either local or distant. Survival curves were estimated using the Kaplan–Meier method, and the differences in survival were evaluated using the long-rank test. Cox's proportional hazards modeling of parameters potentially related to survival was conducted to calculate hazard ratios (HRs), in both univariate and multivariate analyses. All of these statistical analyses were performed using SPSS v20 (SPSS Inc, Chicago, IL, USA) and JMP10 software (SAS Institute Inc, Cary, NC, USA). $p < 0.05$ was considered statistically significant. Statistical analysis of *in vitro* functional assays was performed by using SPSS v20.

Results

YAP1/TAZ are expressed in EwS cell lines and tumor specimens, and are associated with the presence of metastasis and poor prognosis

First, we examined YAP1/TAZ expression by western blotting (WB) in 13 EwS cell lines with different pathognomonic gene fusions (Figure 1A). We observed heterogeneous expression of both proteins across the cell

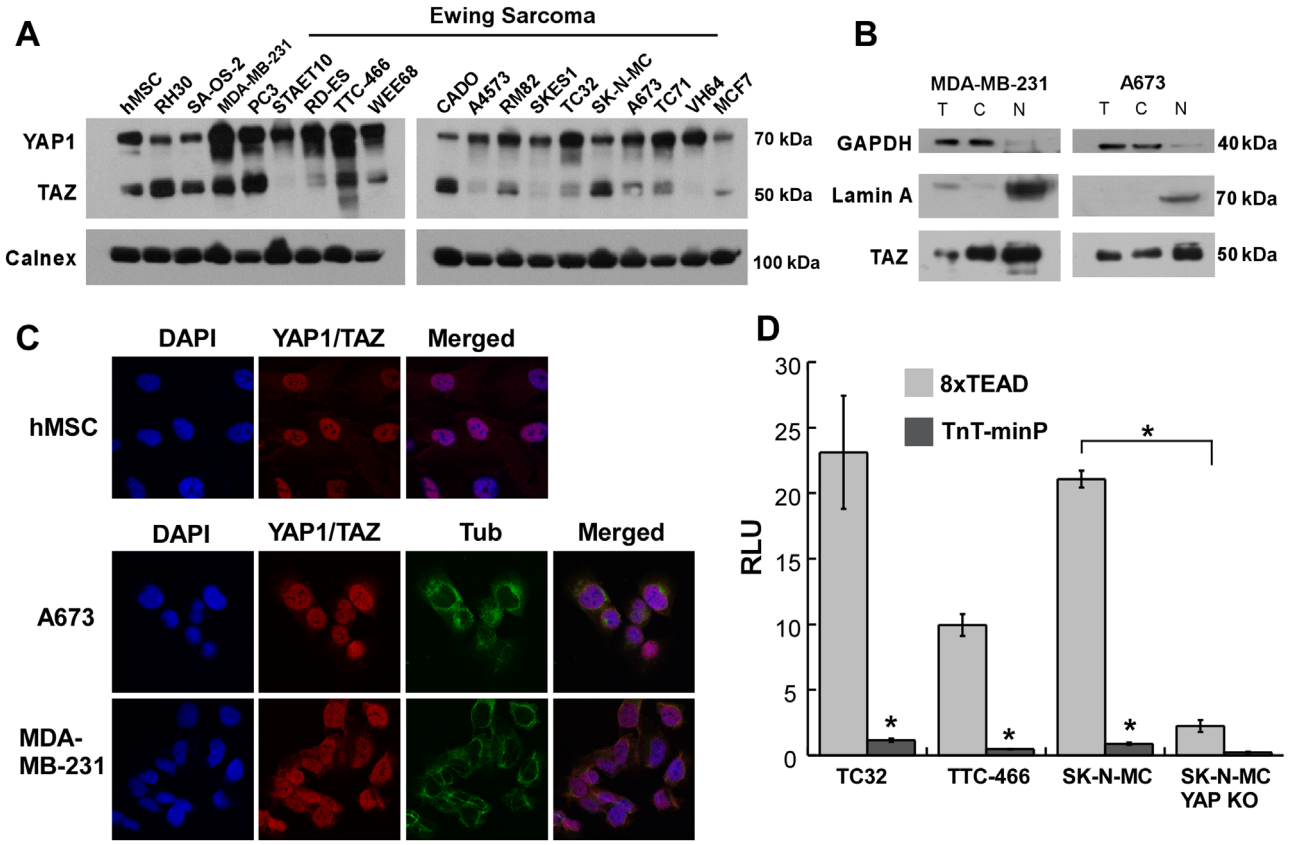

Figure 1. YAP1 and TAZ are expressed and active in EwS cell lines. (A) Western blot using a monoclonal antibody recognizing total levels of YAP1 and TAZ proteins in a panel of 13 EwS cell lines. Basal and luminal breast cancer (MDA-MB-231, MCF-7), prostate cancer (PC3), osteosarcoma (SA-OS-2), rhabdomyosarcoma (RH30), and human mesenchymal stem cells (hMSC) were included in the assay. (B) Nucleus and cytoplasm subcellular lysates were assessed by WB (T, total extract; N, nucleus; C, cytoplasm). (C) Immunofluorescence images using the indicated antibodies (60× original objective magnification). (D) YAP1/TAZ-TEAD-dependent transcriptional activity in EwS cell lines was evaluated with luciferase reporter constructs containing sequences with or without TEAD elements (8×TEAD and TnT-minP constructs, respectively). A Crispr-edited cell line was assessed as an additional negative control (SK-N-MC YAP KO). RLU (relative luminescence units) was normalized to *Renilla* luciferase values. Data are shown as mean ± SEM of three biological replicates (*$p < 0.001$).

line panel. Some of the EwS cell lines showed YAP1/TAZ expression comparable to cell lines in which a relevant role has been described for these factors (i.e. MDA-MB-231, a triple-negative breast cancer cell line with *NF2* mutations leading to activation of YAP1/TAZ) [25]. YAP1/TAZ expression was also detected in human mesenchymal stem cells (hMSCs) derived from bone marrow, a proposed cell of origin of EwS. Importantly, nuclear expression was observed by subcellular fractionation and immunofluorescence (Figure 1B,C and supplementary material, Figure S1), suggesting functional transcriptional activity which was confirmed with luciferase reporter assays (Figure 1D).

To test whether YAP1/TAZ abundance was associated with clinical variables in EwS, we analyzed their expression by IHC in a retrospective series of 55 primary tumors (Table 1). YAP1/TAZ-strong expressing tumor cells exhibited intense nuclear staining with a variable signal in the cytoplasm (Figure 2A). YAP1/TAZ expression was also observed in endothelial cells in negative samples, providing an internal positive control for the IHC determination (Figure 2B). YAP1/TAZ strong expression was associated with disease progression (chi-squared test, $p < 0.0054$), whereas no significant association was observed with age at surgery or location (Table 1). We also observed increased YAP1/TAZ positivity in metastatic or relapsed tumors in 11 patients with paired primary tumor samples (Figure 2C–I, paired *t*-test, $p = 0.0204$). Additional non-paired metastatic or relapsed tumor samples showed preferential strong expression as well (Figure 2J, Fisher's exact test, $p = 0.006$).

We retrieved follow-up data for the EwS patients with primary tumor biopsies to evaluate prognosis (median duration of follow-up 35.23 months), but only 45 had a known relapse date (median duration of follow-up 41.43 months). YAP1/TAZ expression influenced significantly the time to relapse, which was shorter in strong positive patients than in weak/negative patients (mean 127.4 versus 50.66 months, $p = 0.011$, Figure 2K). Similarly, Kaplan–Meier estimates of EwS-specific survival were shorter (but not significantly) for the YAP1/TAZ strong positive group compared with the YAP1/TAZ weak/negative group (mean 129.32 versus 73.61 months, $p = 0.159$, Figure 2L). Accordingly, Cox regression

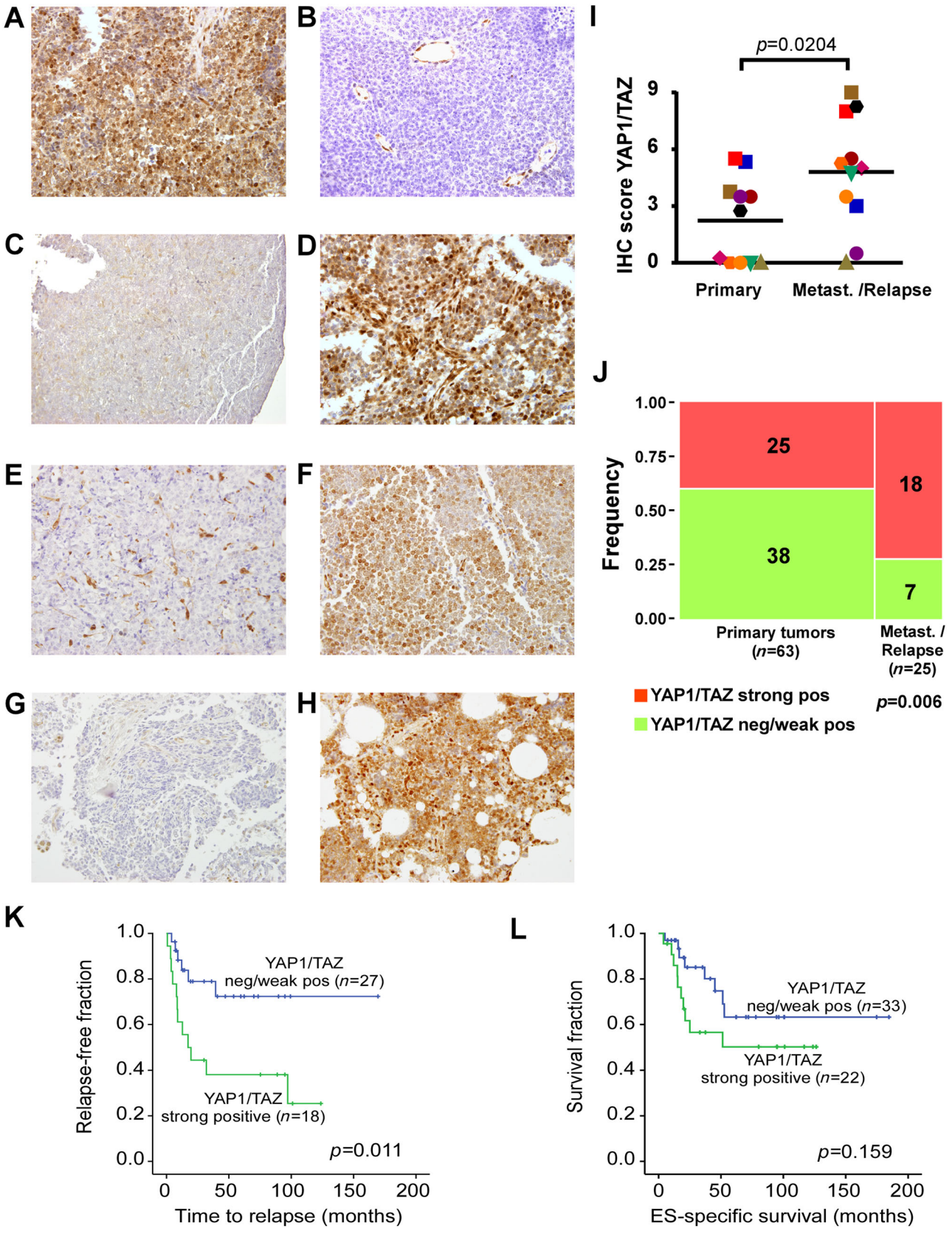

Figure 2. YAP1/TAZ expression is associated with disease progression. (A) Representative image for YAP1/TAZ strong positive expression in a primary EwS tumor (40× original objective magnification). (B) Staining of endothelial cells can be observed in a negative tumor specimen. (C–H) Immunostaining for YAP1/TAZ in primary tumors (left) and matched metastasis (right) of the same patients (40×). (I) Comparison of YAP1/TAZ immunostaining in 11 matched biopsies (p = 0.024, paired t-test). (J) Distribution of samples in each tumor category (primary versus metastasis or relapse) according to YAP1/TAZ staining score. The number of samples is indicated on the bars (p = 0.006, Fisher's exact test). (K, L) Kaplan–Meier survival curves for YAP1/TAZ protein expression in EwS patients grouped as negative/weak positive versus strong positive staining.

Table 2. Prognostic value of YAP1/TAZ IHC expression in relation to other clinical variables

Factors	Time to relapse				EwS-specific survival			
	Unadjusted HR (95% CI)	p	Adjusted HR (95% CI)	p	Unadjusted HR (95% CI)	p	Adjusted HR (95% CI)	p
TAZ/YAP1 (strong versus negative/weak)	3.354 (1.253–8.974)	**0.016**	1.579 (0.287–8.676)	0.599	1.928 (0.761–4.886)	0.167	5.703 (1.004–32.400)	**0.049**
Metastasis	14.895 (4.675–47.455)	**<0.001**	70.369 (4.980–994.326)	**0.002**	11.318 (3.211–39.895)	**<0.001**	77.954 (7.332–828.754)	**<0.001**
Age	0.967 (0.916–1.022)	0.234	1.034 (0.924–.1022)	0.557	0.970 (0.925–1.017)	0.208	0.971 (0.888–1.062)	0.523
Location (bone versus soft tissue)	2.491 (0.667–9.294)	0.174	2.612 (0.468–14.594)	0.274	1.066 (0.326–3.483)	0.916	2.640 (0.478–14.570)	0.265

HR, hazard ratio; CI, confidence interval. *p* numbers in bold highlight significant HR ($p < 0.05$).

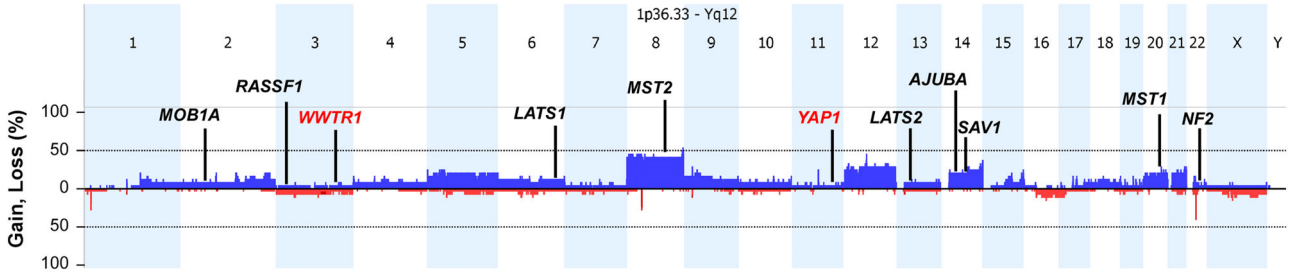

Figure 3. Summary of the copy number aberrations detected in 24 EwS samples. Frequencies of copy number gain (above axis, blue) and copy number loss (below axis, red) across the human genome. Hippo-related loci are indicated: Tumor suppressor genes such as core kinases of the pathway are marked in black, and oncogenes *WWTR1* and *YAP1* in red.

univariate analyses determined that YAP1/TAZ strong expression was significantly correlated with the time to relapse but not with EwS-specific survival, with the unadjusted hazard ratio (HR) being 3.354 ($p = 0.016$) and 1.928 ($p = 0.167$), respectively (Table 2). A significant correlation with survival and time to relapse was also observed for metastasis (Table 2). These variables were all included simultaneously, to assess the independent prognostic significance based on multivariate analysis. The adjusted HR of YAP1/TAZ strong expression for relapse did not reach significant confidence after controlling the Cox's regression model for the effects of age, tumor location, and metastasis. However, a significant HR for YAP1/TAZ was obtained in the multivariate analysis regarding overall survival (Table 2).

Activation of YAP1/TAZ in Ewing sarcoma

We tried to determine the mechanisms that contribute to YAP1/TAZ activation in EwS. We did not find any recurrent somatic mutation in Hippo pathway-related genes in public datasets (supplementary material, Figure S2). Next, we analyzed copy number alterations in a series of 24 EwS using SNP arrays (Figure 3). Gross chromosomal alterations were similar to previous reports, i.e. gains of whole chromosomes 8 and 12 [7]. Copy number gain in the *WWTR1* locus, with complete gain of chromosome 3, was detected in a single case. Gain at the *YAP1* locus was detected in another case with an almost tetraploid genotype. Regarding the core regulatory kinases of the Hippo pathway and other negative regulators of YAP1/TAZ, no significant copy-loss events were observed (Figure 3). Focal copy number aberration events in Hippo-related loci were also precluded after inspecting the data with the STAC algorithm (supplementary material, Table S2). Similarly, Hippo-related loci were unaffected in a retrospective series of 165 cases of EwS, which was analyzed within the PROVABES Consortium for validation of biomarkers in EwS (https://www.medizin.uni-muenster.de/provabes/network, Díaz-Martín J, unpublished data).

Deregulation of the Hippo pathway leading to YAP1/TAZ activation could be the consequence of epigenetic silencing of tumor suppressor genes through DNA hypermethylation [11,15,26]. We inspected previous results of the group comparing CpG methylation in EwS cell lines versus hMSCs from EwS patients and healthy donors (GSE118872) [21]. *RASSF1* was the only Hippo-related locus showing differential methylation (Figure 4A). Hypermethylation of *RASSF1* accounts for the silencing of *RASSF1A* transcript expression, but promotes switching to an alternative gene promoter driving the expression of the isoform *RASSF1C*. *RASSF1A* contributes to Hippo pathway-mediated repression of YAP1/TAZ, whereas *RASSF1C* promotes Src family kinase (SFK)-mediated activation of YAP1 [27]. We confirmed the expression of the alternative isoform *RASSF1C* in EwS cell lines, whereas *RASSF1A*

expression was absent or reduced (with the exception of the STAET-10 and TC-32 cell lines) compared with hMSCs (Figure 4B). Moreover, expression of YAP1/TAZ target genes positively correlated with *RASSF1C* expression in the cell line panel, as well as in EwS tumor specimens (Figure 4B,C). Interestingly, TAZ, but not YAP1, seems to be transcriptionally regulated as *CTGF* expression correlated with *TAZ* mRNA expression (Figure 4C). Correlation of *TAZ* mRNA levels with Hippo target genes was also observed in larger EwS series in public repository expression data (supplementary material, Figure S3).

There is extensive evidence that SFKs can directly phosphorylate YAP1 and TAZ, promoting their activity and stability [28]. Therefore, since *RASSF1C* activates SFKs in *RASSF1*-methylated cells [27], we blocked SFK activity by exposing EwS cells to dasatinib. Inhibition of SFKs, monitored as SRC phosphorylation, resulted in reduced cell viability (SK-N-MC IC_{50} = 6.55 μM; TTC-466 IC_{50} = 2.11 μM) and downregulation of YAP1/TAZ target genes (Figure 5A). Upon dasatinib treatment, the mRNA levels of *YAP1* and *TAZ* remained unaffected, but TAZ protein expression was decreased and YAP1 inactivating phosphorylation S127 increased in both cell lines (Figure 5A). As an alternative approach of pharmacologic blockade of YAP1/TAZ activity, we tested pitavastatin. Statins prevent nuclear localization of YAP1/TAZ via inhibition of the enzyme HMG-CoA reductase, ultimately affecting the metabolic control of YAP1/TAZ by the mevalonate pathway [29]. We also observed an antiproliferative effect upon pitavastatin treatment (SK-N-MC IC_{50} = 1.83 μM; TTC-466 IC_{50} = 1.86 μM), with mild reduction of YAP1/TAZ target genes and TAZ protein downregulation (Figure 5A). Neither dasatinib nor pitavastatin treatments affected EWS–FLI1 expression in the SK-N-MC cell line, thus precluding that the antiproliferative effect of these drugs was mediated by the fusion protein.

YAP1/TAZ loss-of-function affects cell proliferation and invasion capacity in EwS cells

To assess the oncogenic properties of YAP1 and TAZ in EwS cells, we induced transient knockdown of YAP1, TAZ or simultaneous depletion of both factors (supplementary material, Figure S4), and evaluated cell proliferation, invasion, and migration capacity of the silenced cells. We observed inhibition of proliferation for every individual or combined siRNA transfection. Individual depletion of YAP1 inhibited cell growth more efficiently than TAZ silencing (supplementary material, Figure 5B). Accordingly, Crispr-mediated knockout (KO) of YAP1 reduced colony formation *in vitro* and impaired tumor growth in a subcutaneous xenograft model (Figure 5D,E).

YAP1/TAZ silenced cells showed a significantly reduced invasive capacity as well (Figure 5C). The migration capacity of EwS cells upon YAP1/TAZ silencing was not significantly altered compared with the control, but a slight trend toward diminished migration was observed in the double-silenced cells (supplementary material, Figure S5).

YAP1/TAZ-driven transcription activity is inversely correlated with the EWS–FLI1 transcriptional signature

To evaluate the transcriptome modulation by YAP1/TAZ, we conducted gene expression profiling using Affymetrix microarrays in SK-N-MC cells upon simultaneous silencing of both factors. The microarray data have been deposited in the NCBI Gene Expression Omnibus (accession code GSE120512; https://www.ncbi.nlm.nih.gov/geo/query/acc.cgi?acc=GSE120512). We observed differential expression of 938 coding genes (supplementary material, Table S3) including well-established YAP1/TAZ target genes, such as *CYR61*, *CTGF*, and *AMOTL2*, which were confirmed by RT-qPCR analyses in two EwS cell lines with different gene fusions (Figure 6A). Similar results were obtained with individual silencing of each factor (supplementary material, Figure S6). Of note, the expression levels of *EWS–FLI1* were not affected in SK-N-MC (Figure 6A) or other EwS cell lines tested (supplementary material, Figure S6).

Next, we collated this transcriptional profile with previously published curated gene sets. Interestingly, we found significant enrichment for several EwS-related gene signatures both in YAP1/TAZ-correlated and in YAP1/TAZ-inversely correlated genes (Table 3 and Figure 6B). YAP1/TAZ-inversely correlated genes were significantly over-represented among EwS induced gene sets, and YAP1/TAZ-correlated genes overlapped with EwS repressed genes, thus suggesting opposite transcriptional activity of EWS–FLI1 chimeric protein and YAP1/TAZ factors. Accordingly, depletion of the EWS–FLI1 protein in the A673 EwS cell line resulted in the induction of YAP1/TAZ-regulated genes, as well as the TAZ but not the YAP1 factor, the latter showing a slight increase in the phosphorylated fraction (Figure 6C, left and center panels). TAZ protein upregulation upon EWS–FLI1 silencing could be observed in both nuclear and cytoplasmic compartments (Figure 6C, right panel). Therefore, transcriptional antagonism may be explained partially by EWS–FLI1-mediated downregulation of TAZ. We confirmed these observations in public datasets for EWS–FLI1 silencing in five EwS cell lines [30], and for ectopic expression of EWS–FLI1 in embryonic stem cells [31] (supplementary material, Figure S7). These observations are in accordance with recent reports describing that several genes are inversely regulated by TEAD factors and EWS–FLI1 [32,33]. TEADs are the main transcription factor partners of YAP1 and TAZ, and usually associate with AP-1 transcription factors at distal enhancers [25,34]. Both TEAD and AP-1 conserved binding motifs are present in EWS–FLI1 regulated genes [32]. Furthermore, EWS–FLI1 binding at the *WWTR1*

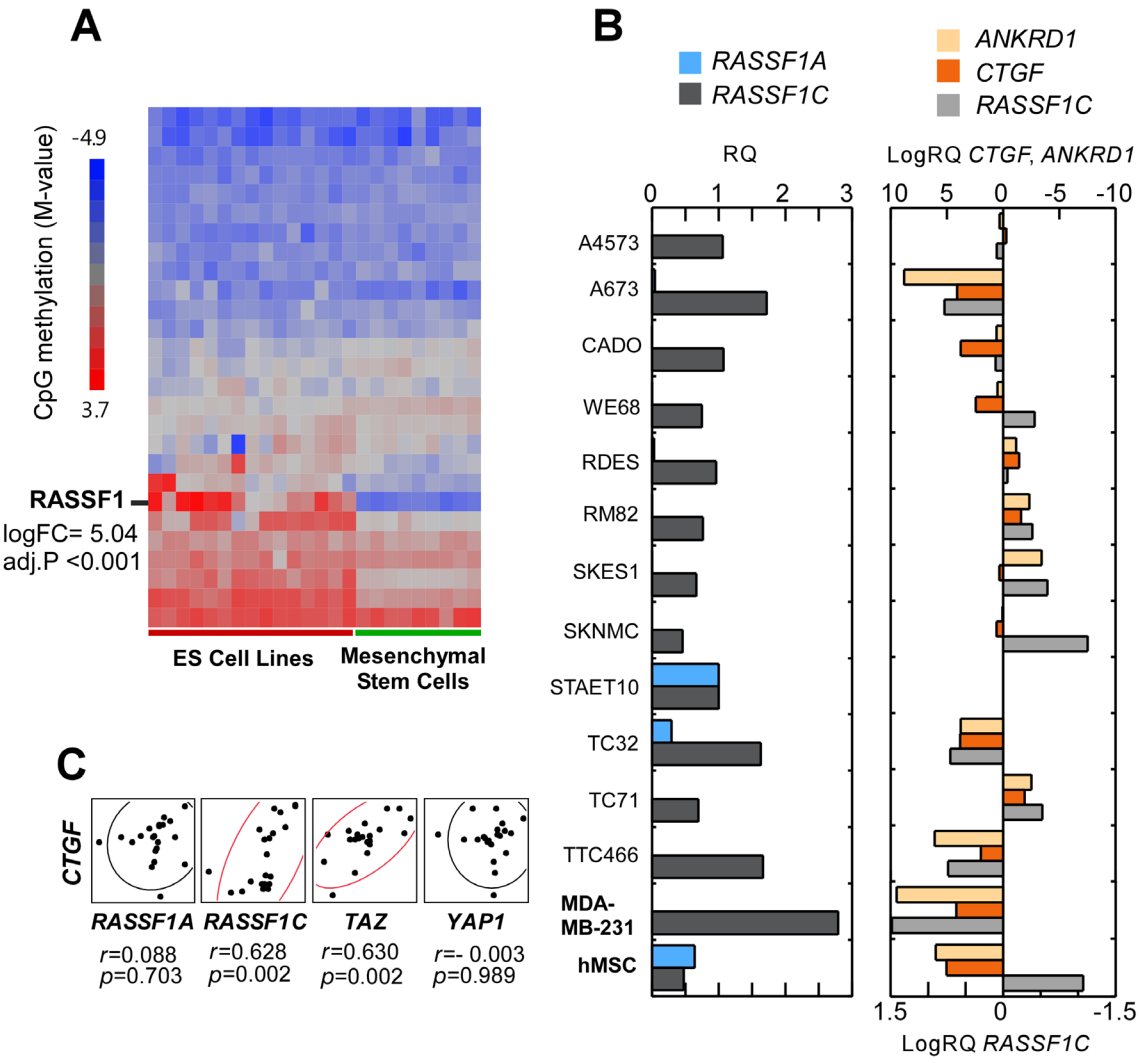

Figure 4. DNA methylation profiling of EwS cell lines and MSCs revealed differential CpG methylation in the *RASSF1* locus. (A) Heat map depicting CpG methylation levels of Hippo-related loci across a panel of EwS cell lines and hMSCs from EwS patients and healthy donors. (B) Relative quantification by RT-qPCR of *RASS1A* and *RASSF1C* transcripts and TAZ/YAP1 target genes in a panel of EwS cell lines. A basal breast cancer cell line and hMSCs were included as controls (experiments were performed with three biological samples in triplicates). (C) Correlation analyses of mRNA expression levels (RT-qPCR) of *CTGF* with *RASSF1C*, *RASSF1A*, *TAZ*, and *YAP1* from a series of 21 frozen EwS tumor specimens (*r*, Pearson's correlation coefficient).

locus coding for TAZ correlates with a decrease of *TAZ* mRNA expression, suggesting direct repression of TAZ by EWS–FLI1 (supplementary material, Figure S8).

Discussion

In the present study, we have shown that YAP1/TAZ nuclear expression is associated with disease progression and poor prognosis in a large retrospective series of EwS patients. Few reports have addressed this issue so far, and the reported series were smaller, i.e. Ahmed *et al* [35] observed that YAP1 expression can be detected in 47% of samples (in a series of 32 cases) without an association with survival, whereas in another study with only five EwS cases, 60% and 80% showed YAP1 and TAZ expression, respectively [36]. Other pediatric sarcomas such as rhabdomyosarcoma, osteosarcoma, and neuroblastoma have been reported to express YAP1 and TAZ, with an impact on patient prognosis and conferring resistance to current therapies [37–41]. Moreover, recent studies have revealed that YAP1/TAZ are key signaling mediators of the oncogenic fusion genes in synovial sarcoma, myxoid liposarcoma, and alveolar rhabdomyosarcoma [42–44]. This positive functional cooperation in translocated sarcomas contrasts with the antagonism between YAP1/TAZ and EWS–FLI1 that we have observed in EwS.

Another fact that supports the relevance of YAP1/TAZ and other Hippo signaling effectors in sarcomas is their involvement in recurrent fusion genes in certain histological types [45,46]. Notwithstanding, aberrant activation of YAP1/TAZ in cancer is often promoted by mechanisms not involving somatic alterations. We have observed that epigenetic regulation of the *RASSF1* locus could affect the expression of YAP1/TAZ target genes in EwS cell lines (Figure 4). This result may explain previous observations describing a correlation of hypermethylation of *RASSF1*

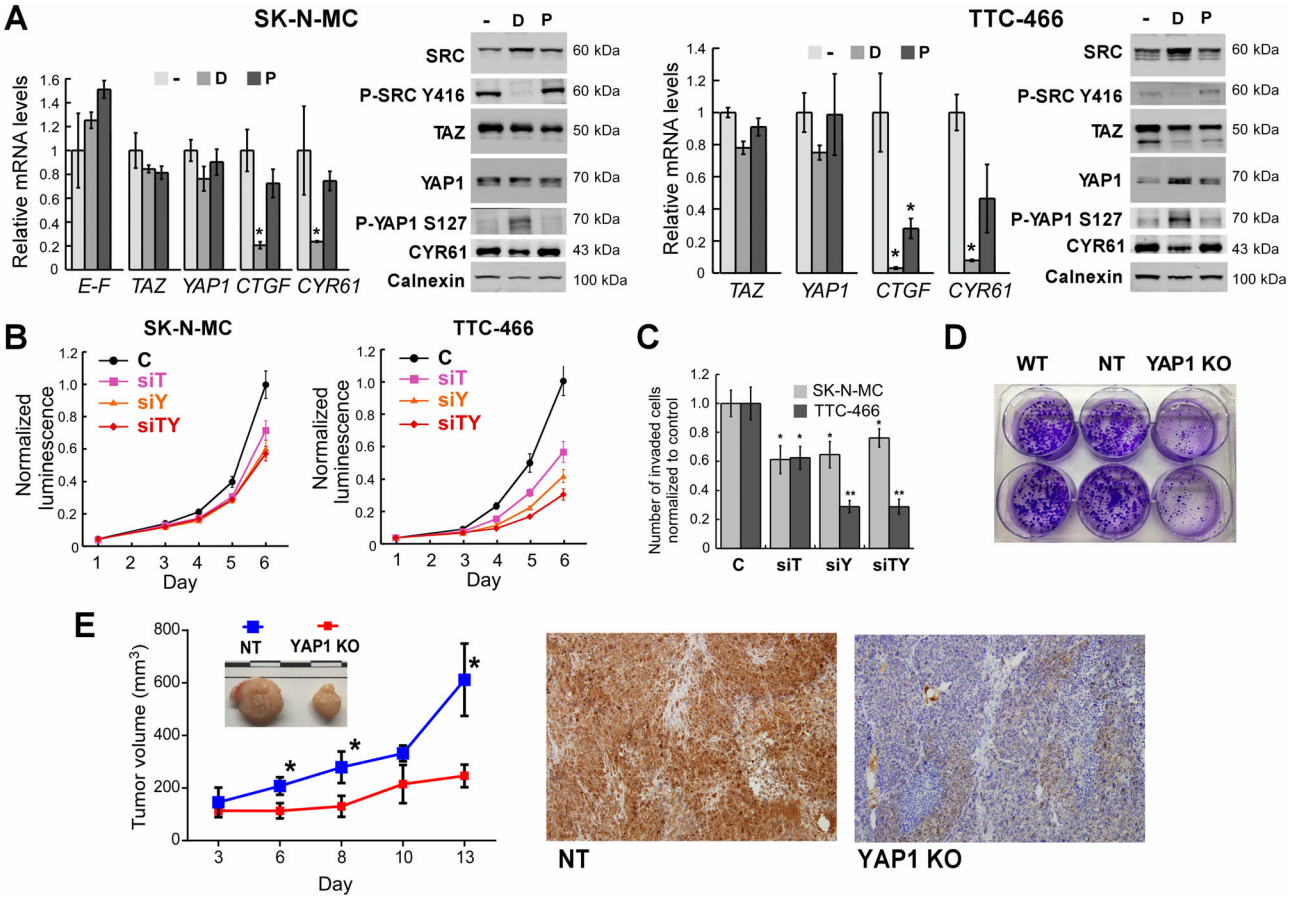

Figure 5. Pharmacologic inhibition and siRNA silencing of YAP1/TAZ in EwS cells. (A) SK-N-MC and TTC-466 cell lines were treated with vehicle (–, DMSO < 1:1000 v/v), dasatinib (D, 1 μM) or pitavastatin (P, 1 μM) during 24 h, and mRNA levels of *YAP1*, *TAZ*, and their target genes *CTGF* and *CYR61* were quantified by RT-qPCR. mRNA levels of *EWS–FLI1* were evaluated in the SK-N-MC cell line. Whole cell extracts were also analyzed by WB (experiments were performed with three biological samples in triplicates; *$p < 0.05$, *t*-test). (B) Proliferation curves of EwS cell lines transfected with control siRNA (C), siRNA targeting *YAP1* (siY), *TAZ* (siT) or a combination of siRNAs to deplete both factors simultaneously (siYT). Two different siRNAs were used to knock down each factor, rendering similar levels of silencing (supplementary material, Figure S4). Data are shown for only one of the siRNAs. Results are shown as mean ± SD of three independent experiments performed in triplicate. All the conditions were significantly different form the control at day 6 ($p < 0.05$, *t*-test). (C) Invasion assay of EwS cell lines upon individual or combined silencing of YAP1 and TAZ (*$p < 0.05$, **$p < 0.005$; *t*-test). (D) Colony formation assay of the SK-N-MC cell line (WT, wild type; NT, non-targeting sgRNA; YAP1 KO, CRISPR-mediated KO of YAP1). (E) Time course of tumor growth in mice with the indicated xenografts.

and *RASSF2* with worse clinical outcome in EwS [47,48]. Moreover, Src kinase activation of invadopodia in response to stress in EwS [49] could be related to SFK-mediated activation of YAP1/TAZ by *RASSF1C* (Figure 5A). However, YAP1/TAZ activation does not seem to rely on *RASSF1* hypermethylation in hMSC (Figure 4), the putative cell of origin of EwS, which exhibits high expression levels of YAP1 and TAZ (Figure 1). Unaffected expression of total levels of YAP1 and derepression of TAZ upon EWS–FLI1 silencing (Figure 6E) also support the notion that both factors are maybe expressed in the cell of origin, as proposed for ZEB2, an EMT (epithelial–mesenchymal transition) inducer like YAP1 and TAZ [50].

The association of YAP1/TAZ with metastatic spread could arguably be related to the relative levels of the fusion protein, recently reported to promote phenotypic plasticity of EwS cells [16]. In this scenario, YAP1/TAZ may promote a mesenchymal phenotype in EWS–FLI1-depleted EwS cells together with Wnt/beta-catenin [51], since it is well established that the crosstalk between Hippo and Wnt signaling is essential for tumor progression in several types of cancer [52]. As has been described for Wnt/beta-catenin [51], the opposing transcriptional signature between YAP1/TAZ and EWS–FLI1 could partly contribute to the metastatic process; i.e. we found strong downregulation or upregulation of *LOX* (a mediator of metastasis [16]) in YAP1/TAZ-silenced or EWS–FLI1-silenced cells, respectively. These results suggest that LOX expression in EwS could be explained by derepression in a low-level state of the fusion protein and/or inducer mechanisms involving YAP1 or TAZ. However, we did not observe differences in LOX expression by IHC in metastatic tumors of eight matched samples, neither did we find differences in FLI1 or NKX2.2 (EWS–FLI induced target) staining in the same matched samples (supplementary Figure S8). Nevertheless, a larger series of paired samples would be necessary to reach a definite conclusion.

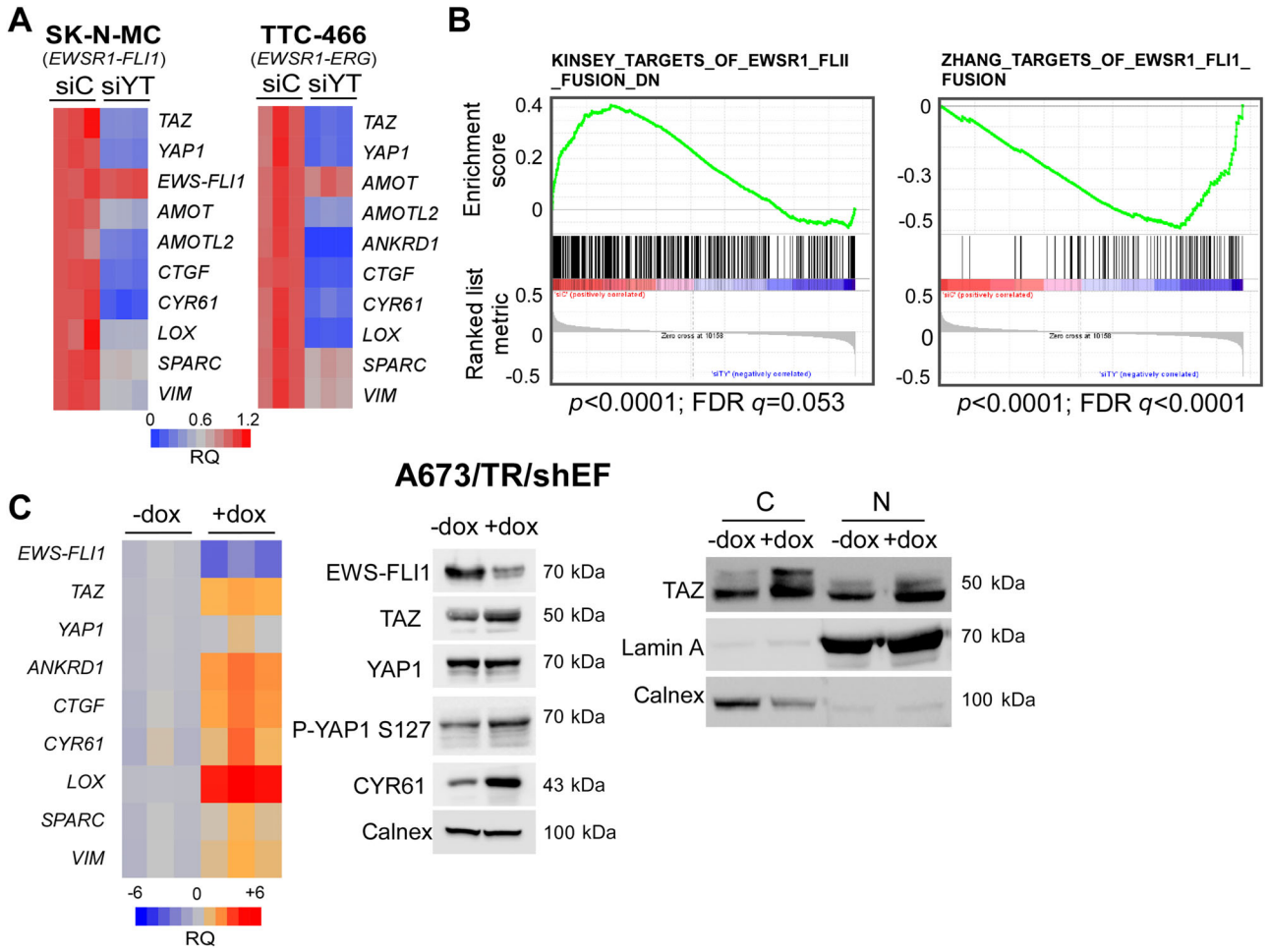

Figure 6. YAP1/TAZ induce an EWS–FLI1-opposite gene signature. (A) RT-qPCR assays for YAP1/TAZ target genes in EwS cell lines with different gene fusions upon siRNA depletion of YAP1 and TAZ (see supplementary material, Figure S6 for RT-qPCR with individual silencing of each factor). Experiments were performed with three biological samples in triplicates. (B) Examples of YAP1/TAZ rank-ordered target genes compared with downregulated and upregulated *EWS–FLI1* gene sets, respectively (NES, normalized enrichment score). (C) RT-qPCR (left) and WB assays (center, right) showing derepression of TAZ and YAP1/TAZ target genes upon silencing of EWS–FLI1 in the cell line A673 (dox, doxycycline induction of shRNA targeting *EWS–FLI1*; C, cytoplasm; N, nucleus). Assays were performed with three biological samples in triplicates.

Table 3. EwS gene sets with a positive and negative enrichment score for YAP1/TAZ regulated genes in the SK-N-MC cell line

Gene set	NES	NOM *P* value	FDR *q* value
KINSEY_TARGETS_OF_EWSR1_FLII_FUSION_DN	1.9	< 0.0001	0.053
ZHANG_TARGETS_OF_EWSR1_FLI1_FUSION	−2.24	< 0.0001	< 0.0001
RIGGI_EWING_SARCOMA_PROGENITOR_UP	−1.97	< 0.0001	0.008
MIYAGAWA_TARGETS_OF_EWSR1_ETS_FUSIONS_UP	−1.84	< 0.0001	0.024
FERREIRA_EWINGS_SARCOMA_UNST_VS_STABLE_UP	−1.73	< 0.0001	0.057

NES, normalized enrichment score.

ChIP-seq data from Bilke *et al* [53] reveal that EWSR1–FLI1 binds at regulatory elements of some of the well-established TAZ/YAP1 target genes [33]. Furthermore, an inverse correlation between AP-1-induced genes and the EWSR1–FLI1 transcriptional signature was observed in the same cell model that we used in this work: inducible silencing of EWSR1–FLI1 in the A673 cell line [33]. It is well established that YAP1/TAZ/TEAD transcriptional complexes usually cooperate with AP-1 at regulatory DNA modules to synergistically activate target genes [25,34]. Therefore, the transcriptional antagonism might be a consequence of some interference between YAP1/TAZ/TEAD–AP1 complexes and the fusion protein, as demonstrated by Katschnig *et al* [32]. Another mechanism contributing to the opposing gene signatures might involve Ewing sarcoma-associated transcript 1 (*EWSAT1*), which we found to be significantly induced in YAP1/TAZ-silenced SK-N-MC cells (supplementary material, Table S3). *EWSAT1* is a long noncoding RNA that mediates *EWS–FLI1* gene repression via interaction with a heterogeneous nuclear ribonucleoprotein [54]. In addition, we have observed inhibition of TAZ expression associated with the presence of EWS–FLI1, which also

binds DNA at the *WWTR1* locus (supplementary material, Figure S9). Indeed, regulation of TAZ seems to occur at the transcriptional level, whereas YAP1 activity is not correlated with mRNA levels (Figures 4C and 6E).

In summary, our study reveals that the interplay between the Hippo pathway effectors YAP1/TAZ and the function of the gene fusion is relevant to shape the transcriptional program in EwS. The transcriptional output elicited by these factors deserves further characterization as our observations provide clinical evidence that YAP1/TAZ expression is associated with disease progression in EwS patients. Studies with larger prospective series are needed in order to corroborate our observations and to establish whether YAP1/TAZ could serve as reliable biomarkers to stratify and identify patients who could benefit from targeted therapies.

Acknowledgements

This research was conducted using samples from the Hospital Universitario Virgen del Rocío-Instituto de Biomedicina de Sevilla Biobank (Andalusian Public Health System Biobank and ISCIII-Red de Biobancos PT17/0015/0041). We thank the donors for the human specimens used in this study. This work was supported by a grant from the Fundación Pública Andaluza Progreso y Salud (Junta de Andalucía) and JANSSEN CILAG, S.A. (grant No PI-0344-2014) to JDM. PRN is a PhD student recipient of a PFIS fellowship to Enrique de Alava (grant No F109/00193). JDM, LRP, and ATM are PhD researchers funded by the Asociación Española Contra el Cáncer (AECC, GCB13-1578). CJ works as a laboratory technician supported by the ISCIII. EDA's laboratory is supported by the AECC project (GCB13-1578), ISCIII-FEDER (PI14/01466, PI17/00464), CIBERONC (CB16/12/00361), Asociación Pablo Ugarte, and Fundación María García Estrada. The laboratory of TGPG is supported by the 'Verein zur Förderung von Wissenschaft und Forschung an der Medizinischen Fakultät der LMU München' (WiFoMed), by LMU Munich's Institutional Strategy LMUexcellent within the framework of the German Excellence Initiative, the 'Mehr LEBEN für krebskranke Kinder – Bettina-Bräu-Stiftung' to TGPG, the Kind-Philipp-Foundation, the Matthias-Lackas Foundation, the Dr Rolf M Schwiete Foundation, the Dr Leopold and Carmen Ellinger Foundation, the Wilhelm-Sander-Foundation (2016.167.1), the German Cancer Aid (DKH-70112257), the Gert und Susanna Mayer Foundation, and the Deutsche Forschungsgemeinschaft (DFG-391665916). JA's laboratory is supported by Instituto de Salud Carlos III (PI16CIII/00026, DTS18CIII/00005), Asociación Pablo Ugarte (TPY-M 1149/13; TRPV 205/18), ASION (TVP 141/17), Fundación Sonrisa de Alex, and Todos somos Iván (TVP 1324/15). We thank Dr Stefano Piccolo for the luciferase reporter plasmid with TEAD motifs (Addgene plasmid # 34615), Dr Mark Bond for providing the plasmid pTNT-min, and Dr Campana for the hMSC TERT cell line.

Author contributions statement

JDM, PRN, and LRP contributed equally to this work and were responsible for the experimental design and the undertaking of the experiments. EA and DM reviewed the pathological and immunohistochemical analyses, and the clinical data. ATM, PPC, and CJ carried out some of the experiments. JDM, JA, LRP, and PRN performed the statistical analysis and interpreted the data. TGPG analyzed public datasets. JDM designed the study, and LRP, EA, and JDM were involved in writing the paper. JDM generated the figures and drafted the manuscript. All the authors contributed to the editing of the manuscript and gave their approval of the final version.

Data availability statement

Our microarray data have been deposited in the NCBI Gene Expression Omnibus as GSE120512 (https://www.ncbi.nlm.nih.gov/geo/query/acc.cgi?acc=GSE120512).

References

1. Choi EY, Gardner JM, Lucas DR, *et al*. Ewing sarcoma. *Semin Diagn Pathol* 2014; **31:** 39–47.
2. Grunewald TGP, Cidre-Aranaz F, Surdez D, *et al*. Ewing sarcoma. *Nat Rev Dis Primers* 2018; **4:** 5.
3. Gorlick R, Janeway K, Lessnick S, *et al*. Children's Oncology Group's 2013 blueprint for research: Bone tumors. *Pediatr Blood Cancer* 2013; **60:** 1009–1015.
4. Delattre O, Zucman J, Plougastel B, *et al*. Gene fusion with an ETS DNA-binding domain caused by chromosome translocation in human tumours. *Nature* 1992; **359:** 162–165.
5. Le Deley MC, Delattre O, Schaefer KL, *et al*. Impact of EWS-ETS fusion type on disease progression in Ewing's sarcoma/peripheral primitive neuroectodermal tumor: prospective results from the cooperative Euro-E.W.I.N.G. 99 trial. *J Clin Oncol* 2010; **28:** 1982–1988.
6. Crompton BD, Stewart C, Taylor-Weiner A, *et al*. The genomic landscape of pediatric Ewing sarcoma. *Cancer Discov* 2014; **4:** 1326–1341.
7. Tirode F, Surdez D, Ma X, *et al*. Genomic landscape of Ewing sarcoma defines an aggressive subtype with co-association of *STAG2* and *TP53* mutations. *Cancer Discov* 2014; **4:** 1342–1353.
8. Mackintosh C, Ordonez JL, Garcia-Dominguez DJ, *et al*. 1q gain and CDT2 overexpression underlie an aggressive and highly proliferative form of Ewing sarcoma. *Oncogene* 2012; **31:** 1287–1298.
9. Dong J, Feldmann G, Huang J, *et al*. Elucidation of a universal size-control mechanism in *Drosophila* and mammals. *Cell* 2007; **130:** 1120–1133.

10. Zhao B, Tumaneng K, Guan KL. The Hippo pathway in organ size control, tissue regeneration and stem cell self-renewal. *Nat Cell Biol* 2011; **13:** 877–883.
11. Deel MD, Li JJ, Crose LE, *et al*. A review: molecular aberrations within Hippo signaling in bone and soft-tissue sarcomas. *Front Oncol* 2015; **5:** 190.
12. Barron DA, Kagey JD. The role of the Hippo pathway in human disease and tumorigenesis. *Clin Transl Med* 2014; **3:** 25.
13. Harvey KF, Zhang X, Thomas DM. The Hippo pathway and human cancer. *Nat Rev Cancer* 2013; **13:** 246–257.
14. Ahmed AA, Mohamed AD, Gener M, *et al*. YAP and the Hippo pathway in pediatric cancer. *Mol Cell Oncol* 2017; **4:** e1295127.
15. Johnson R, Halder G. The two faces of Hippo: targeting the Hippo pathway for regenerative medicine and cancer treatment. *Nat Rev Drug Discov* 2014; **13:** 63–79.
16. Franzetti GA, Laud-Duval K, van der Ent W, *et al*. Cell-to-cell heterogeneity of EWSR1-FLI1 activity determines proliferation/migration choices in Ewing sarcoma cells. *Oncogene* 2017; **36:** 3505–3514.
17. Jo VY, Fletcher CD. WHO classification of soft tissue tumours: an update based on the 2013 (4th) edition. *Pathology* 2014; **46:** 95–104.
18. Ottaviano L, Schaefer KL, Gajewski M, *et al*. Molecular characterization of commonly used cell lines for bone tumor research: a trans-European EuroBoNet effort. *Genes Chromosomes Cancer* 2010; **49:** 40–51.
19. Mihara K, Imai C, Coustan-Smith E, *et al*. Development and functional characterization of human bone marrow mesenchymal cells immortalized by enforced expression of telomerase. *Br J Haematol* 2003; **120:** 846–849.
20. Carrillo J, Garcia-Aragoncillo E, Azorin D, *et al*. Cholecystokinin down-regulation by RNA interference impairs Ewing tumor growth. *Clin Cancer Res* 2007; **13:** 2429–2440.
21. Puerto-Camacho P, Amaral AT, Lamhamedi-Cherradi SE, *et al*. Preclinical efficacy of endoglin-targeting antibody–drug conjugates for the treatment of Ewing sarcoma. *Clin Cancer Res* 2019; **25:** 2228–2240.
22. Du P, Kibbe WA, Lin SM. lumi: a pipeline for processing Illumina microarray. *Bioinformatics* 2008; **24:** 1547–1548.
23. Subramanian A, Tamayo P, Mootha VK, *et al*. Gene set enrichment analysis: a knowledge-based approach for interpreting genome-wide expression profiles. *Proc Natl Acad Sci U S A* 2005; **102:** 15545–15550.
24. Mootha VK, Lindgren CM, Eriksson KF, *et al*. PGC-1α-responsive genes involved in oxidative phosphorylation are coordinately downregulated in human diabetes. *Nat Genet* 2003; **34:** 267–273.
25. Zanconato F, Forcato M, Battilana G, *et al*. Genome-wide association between YAP/TAZ/TEAD and AP-1 at enhancers drives oncogenic growth. *Nat Cell Biol* 2015; **17:** 1218–1227.
26. Sanchez-Vega F, Mina M, Armenia J, *et al*. Oncogenic signaling pathways in The Cancer Genome Atlas. *Cell* 2018; **173:** 321–337 e310.
27. Vlahov N, Scrace S, Soto MS, *et al*. Alternate RASSF1 transcripts control SRC activity, E-cadherin contacts, and YAP-mediated invasion. *Curr Biol* 2015; **25:** 3019–3034.
28. Warren JSA, Xiao Y, Lamar JM. YAP/TAZ activation as a target for treating metastatic cancer. *Cancers (Basel)* 2018; **10:** 115.
29. Sorrentino G, Ruggeri N, Specchia V, *et al*. Metabolic control of YAP and TAZ by the mevalonate pathway. *Nat Cell Biol* 2014; **16:** 357–366.
30. Kauer M, Ban J, Kofler R, *et al*. A molecular function map of Ewing's sarcoma. *PLoS One* 2009; **4:** e5415.
31. Gordon DJ, Motwani M, Pellman D. Modeling the initiation of Ewing sarcoma tumorigenesis in differentiating human embryonic stem cells. *Oncogene* 2016; **35:** 3092–3102.
32. Katschnig AM, Kauer MO, Schwentner R, *et al*. EWS-FLI1 perturbs MRTFB/YAP-1/TEAD target gene regulation inhibiting cytoskeletal autoregulatory feedback in Ewing sarcoma. *Oncogene* 2017; **36:** 5995–6005.
33. Tomazou EM, Sheffield NC, Schmidl C, *et al*. Epigenome mapping reveals distinct modes of gene regulation and widespread enhancer reprogramming by the oncogenic fusion protein EWS-FLI1. *Cell Rep* 2015; **10:** 1082–1095.
34. Liu X, Li H, Rajurkar M, *et al*. Tead and AP1 coordinate transcription and motility. *Cell Rep* 2016; **14:** 1169–1180.
35. Ahmed AA, Abedalthagafi M, Anwar AE, *et al*. Akt and Hippo pathways in Ewing's sarcoma tumors and their prognostic significance. *J Cancer* 2015; **6:** 1005–1010.
36. Fullenkamp CA, Hall SL, Jaber OI, *et al*. TAZ and YAP are frequently activated oncoproteins in sarcomas. *Oncotarget* 2016; **7:** 30094–30108.
37. Mohamed A, Sun C, De Mello V, *et al*. The Hippo effector TAZ (*WWTR1*) transforms myoblasts and TAZ abundance is associated with reduced survival in embryonal rhabdomyosarcoma. *J Pathol* 2016; **240:** 3–14.
38. Tremblay AM, Missiaglia E, Galli GG, *et al*. The Hippo transducer YAP1 transforms activated satellite cells and is a potent effector of embryonal rhabdomyosarcoma formation. *Cancer Cell* 2014; **26:** 273–287.
39. Bouvier C, Macagno N, Nguyen Q, *et al*. Prognostic value of the Hippo pathway transcriptional coactivators YAP/TAZ and β1-integrin in conventional osteosarcoma. *Oncotarget* 2016; **7:** 64702–64710.
40. Schramm A, Koster J, Assenov Y, *et al*. Mutational dynamics between primary and relapse neuroblastomas. *Nat Genet* 2015; **47:** 872–877.
41. Deel MD, Slemmons KK, Hinson AR, *et al*. The transcriptional coactivator TAZ is a potent mediator of alveolar rhabdomyosarcoma tumorigenesis. *Clin Cancer Res* 2018; **24:** 2616–2630.
42. Isfort I, Cyra M, Elges S, *et al*. SS18–SSX-dependent YAP/TAZ signaling in synovial sarcoma. In *Clin Cancer Res*. 2019; **25**: 3718–3731.
43. Trautmann M, Cheng YY, Jensen P, *et al*. Requirement for YAP1 signaling in myxoid liposarcoma. *EMBO Mol Med* 2019; **11:** e9889.
44. Crose LE, Galindo KA, Kephart JG, *et al*. Alveolar rhabdomyosarcoma-associated *PAX3–FOXO1* promotes tumorigenesis via Hippo pathway suppression. *J Clin Invest* 2014; **124:** 285–296.
45. Schaefer IM, Fletcher CDM. Recent advances in the diagnosis of soft tissue tumours. *Pathology* 2018; **50:** 37–48.
46. Suurmeijer AJH, Kao YC, Antonescu CR. New advances in the molecular classification of pediatric mesenchymal tumors. *Genes Chromosomes Cancer* 2019; **58:** 100–110.
47. Gharanei S, Brini AT, Vaiyapuri S, *et al*. *RASSF2* methylation is a strong prognostic marker in younger age patients with Ewing sarcoma. *Epigenetics* 2013; **8:** 893–898.
48. Avigad S, Shukla S, Naumov I, *et al*. Aberrant methylation and reduced expression of *RASSF1A* in Ewing sarcoma. *Pediatr Blood Cancer* 2009; **53:** 1023–1028.
49. Bailey KM, Airik M, Krook MA, *et al*. Micro-environmental stress induces Src-dependent activation of invadopodia and cell migration in Ewing sarcoma. *Neoplasia* 2016; **18:** 480–488.
50. Wiles ET, Bell R, Thomas D, *et al*. ZEB2 represses the epithelial phenotype and facilitates metastasis in Ewing sarcoma. *Genes Cancer* 2013; **4:** 486–500.
51. Pedersen EA, Menon R, Bailey KM, *et al*. Activation of Wnt/β-catenin in Ewing sarcoma cells antagonizes EWS/ETS function and promotes phenotypic transition to more metastatic cell states. *Cancer Res* 2016; **76:** 5040–5053.
52. Noguchi S, Saito A, Nagase T. YAP/TAZ signaling as a molecular link between fibrosis and cancer. *Int J Mol Sci* 2018; **19:** 3674.

53. Bilke S, Schwentner R, Yang F, *et al*. Oncogenic ETS fusions deregulate E2F3 target genes in Ewing sarcoma and prostate cancer. *Genome Res* 2013; **23:** 1797–1809.
54. Marques Howarth M, Simpson D, Ngok SP, *et al*. Long noncoding RNA *EWSAT1*-mediated gene repression facilitates Ewing sarcoma oncogenesis. *J Clin Invest* 2014; **124:** 5275–5290.
*55. Dupont S, Morsut L, Aragona M, *et al*. Role of YAP/TAZ in mechanotransduction. *Nature* 2011; **474:** 179–183.
*56. Kimura TE, Duggirala A, Smith MC, *et al*. The Hippo pathway mediates inhibition of vascular smooth muscle cell proliferation by cAMP. *J Mol Cell Cardiol* 2016; **90:** 1–10.
*57. Moreno-Bueno G, Peinado H, Molina P, *et al*. The morphological and molecular features of the epithelial-to-mesenchymal transition. *Nat Protoc* 2009; **4:** 1591–1613.
*58. Schneider CA, Rasband WS, Eliceiri KW. NIH image to ImageJ: 25 years of image analysis. *Nat Methods* 2012; **9:** 671–675.
*59. Postel-Vinay S, Veron AS, Tirode F, *et al*. Common variants near *TARDBP* and *EGR2* are associated with susceptibility to Ewing sarcoma. *Nat Genet* 2012; **44:** 323–327.
*Cited only in supplementary material.

SUPPLEMENTARY MATERIAL ONLINE

Supplementary materials and methods

Figure S1. Immunofluorescence microscopy with the indicated antibodies (60× objective magnification)

Figure S2. Hippo pathway-associated genes do not harbor recurrent mutations in EwS cell lines and patients

Figure S3. *WWTR1* (*TAZ*) expression correlates with EWS–FLI1 targets in EwS patients

Figure S4. Western blotting assay to test silencing of YAP1 and TAZ in the SK-N-MC cell line with two different siRNAs in individual or double transfection

Figure S5. Representative images of a wound healing assay using control or YAP1/TAZ-silenced TTC-466 cells

Figure S6. (A) RT-qPCR quantification of YAZ1/TAZ target genes in the SK-N-MC cell line upon siRNA silencing of *YAP1* and *TAZ*. (B) Lysates from TC-32 and SK-N-MC silenced cells were probed with anti-FLI1 to evaluate EWS–FLI1 protein expression

Figure S7. EWS–FLI1 modulates WWTR1 (TAZ) and Hippo target gene expression in different *in vitro* models

Figure S8. Comparison of YAP1/TAZ, FLI1, NKX2.2, and LOX immunostaining in primary versus metastatic/relapsed samples of matched biopsies

Figure S9. Genome browser screenshot of the *WWTR1* locus showing RNA expression upon inducible silencing of EWS–FLI in the A673 cell line

Table S1. Antibodies, suppliers and dilutions, siRNAs, and qPCR primers

Table S2. STAC peaks identified in 24 EwS samples

Table S3. Genes modulated by YAP1/TAZ (siControl versus siYAP1/TAZ)